

# Origin of quantum-mechanical complementarity probed by a ‘which-way’ experiment in an atom interferometer

S. Dürr, T. Nonn & G. Rempe

Fakultät für Physik, Universität Konstanz, 78457 Konstanz, Germany

**The principle of complementarity refers to the ability of quantum-mechanical entities to behave as particles or waves under different experimental conditions. For example, in the famous double-slit experiment, a single electron can apparently pass through both apertures simultaneously, forming an interference pattern. But if a ‘which-way’ detector is employed to determine the particle’s path, the interference pattern is destroyed. This is usually explained in terms of Heisenberg’s uncertainty principle, in which the acquisition of spatial information increases the uncertainty in the particle’s momentum, thus destroying the interference. Here we report a which-way experiment in an atom interferometer in which the ‘back action’ of path detection on the atom’s momentum is too small to explain the disappearance of the interference pattern. We attribute it instead to correlations between the which-way detector and the atomic motion, rather than to the uncertainty principle.**

In classical physics, a particle moves along a well-defined trajectory. A quantum object, however, reveals its wave character in interference experiments in which the object seems to move from one place to another along several different paths simultaneously. It is essential that these ways are indistinguishable, because any attempt to observe which way the object actually took unavoidably destroys the interference pattern.

The usual explanation for the loss of interference in a which-way experiment is based on Heisenberg’s position–momentum uncertainty relation. This has been illustrated in famous *gedanken* experiments like Einstein’s recoiling slit<sup>1</sup> or Feynman’s light microscope<sup>2</sup>. In the light microscope, electrons are illuminated with light immediately after they have passed through a double slit with slit separation  $d$ . A scattered photon localizes the electron with a position uncertainty of the order of the light wavelength,  $\Delta z \approx \lambda_{\text{light}}$ . Owing to Heisenberg’s position–momentum uncertainty relation, this localization must produce a momentum uncertainty of the order of  $\Delta p_z \approx h/\lambda_{\text{light}}$ . This momentum uncertainty arises from the momentum kick transferred by the scattered photon. For  $\lambda_{\text{light}} < d$ , which-way information is obtained, but the momentum kick is so large that it completely washes out the spatial interference pattern.

However, Scully *et al.*<sup>3</sup> have recently proposed a new *gedanken* experiment, where the loss of the interference pattern in an atomic beam is not related to Heisenberg’s position–momentum uncertainty relation. Instead, the correlations between the which-way detector and the atomic beams are responsible for the loss of interference fringes.

Such correlations had already been studied experimentally. They are, for example, responsible for the lack of ground-state quantum beats in time-resolved fluorescence spectroscopy<sup>4</sup>. Other examples are neutron interferometers, where which-way information can be stored by selectively flipping the neutron spin in one arm of the interferometer<sup>5,6</sup>.

Nevertheless, the *gedanken* experiment of Scully *et al.* was criticized by Storey *et al.*<sup>7</sup>, who argued that the uncertainty relation always enforces recoil kicks sufficient to wash out the fringes. This started a controversial discussion<sup>8–11</sup> about the following question: “Is complementarity more fundamental than the uncertainty

principle?”<sup>10</sup>. This motivated Wiseman *et al.*<sup>10,11</sup> to investigate what constitutes a momentum transfer in a double-slit experiment. They call the usual momentum transfer, like that in Feynman’s light microscope, a “classical” kick; in addition, they define the concept of “quantum” momentum transfer. They find that the loss of interference need not be due to “classical” kicks. In this case the “quantum” momentum transfer cannot be less than that required by the uncertainty principle, so that these “quantum” kicks wash out the fringes.

In this context, Eichmann *et al.*<sup>12</sup> performed an experiment with a light interferometer, where the double slit is replaced by two trapped ions, which can store which-way information in internal states. This scheme was criticized<sup>9</sup>, because the ions play a double role: they act as sources of elementary waves (just like a double slit) and simultaneously as a which-way detector. Hence the momentum transfer from the double slit and the which-way detector cannot be separated.

Here we report on a which-way experiment with an atom interferometer. A microwave field is used to store the which-way information in internal atomic states. We study the mechanical effect of the which-way detection on the atomic centre-of-mass motion separately, and find that the “classical” momentum kicks are much too small to wash out the interference pattern. Instead, correlations between the which-way detector and the atomic motion destroy the interference fringes. We show that the back action onto the atomic momentum implied by Heisenberg’s position–momentum uncertainty relation cannot explain the loss of interference.

## The atom interferometer

Figure 1 shows a scheme of our atom interferometer. An incoming beam of atoms passes through two separated standing wave light beams. The detuning of the light frequency from the atomic resonance,  $\Delta = \omega_{\text{light}} - \omega_{\text{atom}}$ , is large so that spontaneous emission can be neglected. The light fields each create a conservative potential  $U$  for the atoms, the so-called light shift, with  $U \propto I/\Delta$ , where  $I$  is the light intensity (see, for example, ref. 13). In a standing wave the light intensity is a function of position,  $I(z) = I_0 \cos^2(k_{\text{light}} z)$ , where  $k_{\text{light}}$  is the wavevector of the light. Hence the light shift potential takes the form  $U(z) = U_0 \cos^2(k_{\text{light}} z)$ , with  $U_0 \propto I_0/\Delta$ .

The atoms are Bragg-reflected from this periodic potential, if they enter the standing light wave at a Bragg angle (see, for example, ref. 14). This process is similar to Bragg reflection of X-rays from the periodic structure of a solid-state crystal, but with the role of matter and light exchanged. In our experiment, the light creates the periodic structure, from which the matter wave is reflected.

The standing light wave splits the incoming atomic beam A (see Fig. 1) into two beams, a transmitted beam C and a first-order Bragg-reflected beam B. The angle between the beams B and C corresponds to a momentum transfer of exactly  $2\hbar k_{\text{light}}$ , as determined by the spatial period of  $U(z)$ . By varying the light intensity, the fraction of reflected atoms can be adjusted to any arbitrary value. In our experiment, the reflectivity of the beam splitter is tuned to  $\sim 50\%$ .

After switching off the first standing light wave, the two beams are allowed to propagate freely for a time interval  $t_{\text{sep}}$ . During this time, beam B moves a horizontal distance  $d/2$  to the left and beam C moves  $d/2$  to the right. The longitudinal velocities (vertical in Fig. 1) of the two beams are not affected by the light field. Then a second standing light wave is switched on, which also serves as a 50% beam splitter. Now two atomic beams D and E are travelling to the left, while beams F and G are travelling to the right. In the far field, each pair of overlapping beams produces a spatial interference pattern. The fringe period is the same as in a double-slit experiment with slit separation  $d$ . The relevant wavelength is the de Broglie wavelength associated with the momentum of the atoms. The envelope of the fringe pattern is given by the collimation properties of the initial atomic beam A.

The experiment is performed with the apparatus described in ref. 15:  $^{85}\text{Rb}$  atoms are loaded into a magneto-optical trap (MOT). After trapping and cooling, the cloud of atoms is released and falls freely through the apparatus. The resulting pulsed atomic beam is collimated with a mechanical slit 20 cm below the MOT. The atoms then pass the interaction region with the standing light wave inside a microwave resonator. In the far field of the interaction region, 45 cm below the MOT, the atomic position distribution is observed by exciting the atoms with a resonant laser beam and detecting the fluorescence photons. The interaction time  $t_{\text{Bragg}}$  of the atoms with the standing light wave is controlled by switching the light on and off. The small atomic velocity of  $2 \text{ m s}^{-1}$  in the

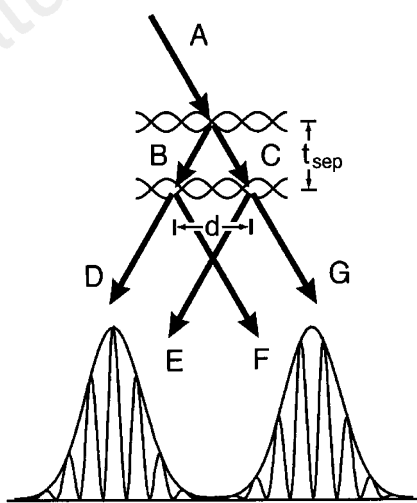


**Figure 1** Scheme of the atom interferometer. The incoming atomic beam A is split into two beams: beam C is transmitted and beam B is Bragg-reflected from a standing light wave. The beams are not exactly vertical, because a Bragg condition must be fulfilled. After free propagation for a time  $t_{\text{sep}}$  the beams are displaced by a distance  $d$ . Then the beams are split again with a second standing light wave. In the far field, a spatial interference pattern is observed.

interaction region allows us to perform the whole interferometer experiment with only one standing light wave, which is switched on and off twice. As compared to ref. 15, only a few changes have been made. The width of the collimation slit was enlarged to 450  $\mu\text{m}$ . In order to improve the position resolution, the horizontal waist of the detection laser beam was reduced to  $w = 50 \mu\text{m}$ , and a second collimation slit with a width of 100  $\mu\text{m}$  was added 1 cm below the MOT. Finally, the preparation of the internal atomic state was improved by removing atoms in wrong Zeeman sublevels.

Figure 2 shows the spatial fringe pattern in the far field for two different values of  $t_{\text{sep}}$ . We note that the observed far-field position distribution is a picture of the atomic transverse momentum distribution after the interaction.

### Storing which-way information

A second quantum system is now added to the interferometer in order to store the information whether the atom moved along way B

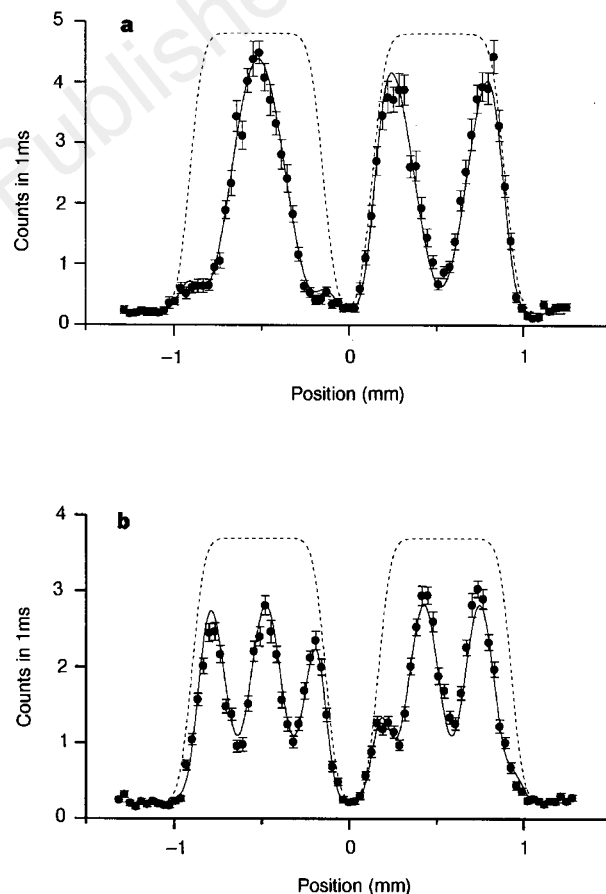


**Figure 2** Spatial fringe pattern in the far field of the interferometer. The data were obtained with  $t_{\text{Bragg}} = 45 \mu\text{s}$ , and the 50% beam splitter was realized with  $|U_0| = \hbar\pi/t_{\text{Bragg}}$ . We chose  $t_{\text{sep}} = 105 \mu\text{s}$  with  $d = 1.3 \mu\text{m}$  (**a**), and  $t_{\text{sep}} = 255 \mu\text{s}$  with  $d = 3.1 \mu\text{m}$  (**b**). In both cases, the fringe period is in good agreement with the theoretical expectation. Each solid line represents a fit to the experimental data. The best-fit values for the visibilities are  $(75 \pm 1)\%$  and  $(44 \pm 1)\%$ , respectively. The reduced visibility for the case of the narrow fringes is due to the finite position resolution of our apparatus. The dashed lines represent the independently measured beam envelope, which consists of two broad peaks. The right peak is due to beams F and G (see Fig. 1), with a shape determined by the momentum distribution of the initial beam A. The left peak is a combination of beams D and E. It is a Bragg-reflected picture of the right peak. The fringe patterns under these two broad peaks are complementary, that is, the interference maxima in the left peak correspond to interference minima in the right peak, and vice versa.

or C. Two internal electronic states of the atom are used as a which-way detector system. A simplified level scheme of  $^{85}\text{Rb}$  is shown in Fig. 3a. Rabi oscillations between states  $|2\rangle$  and  $|3\rangle$  can be induced by applying a microwave field at  $\sim 3$  GHz. To describe the information storing process, we first investigate the properties of one single Bragg beam splitter, using a simple model, whose validity will be discussed later.

The frequency of the standing light wave,  $\omega_{\text{light}}$ , is tuned halfway between the  $|2\rangle \rightarrow |e\rangle$  and  $|3\rangle \rightarrow |e\rangle$  transitions. Hence the detunings from these transitions,  $\Delta_{2e}$  and  $\Delta_{3e}$ , have the same absolute value but opposite sign. The reflectivity of the beam splitter, that is, the probability of reflecting an atom, depends on  $t_{\text{Bragg}} \times |U_0|$ , and it is independent of the internal state.

However, the amplitude of the wavefunction experiences a phase shift which depends on the internal atomic state. A simple analogy for this phase shift can be found in light optics: a light wave reflected from an optically thicker medium experiences a phase shift of  $\pi$ , while reflection from an optically thinner medium or transmission into an arbitrary medium does not cause any phase shift. This argument also applies in atom optics: in our experiment, an atom in  $|2\rangle$  sees a negative light shift potential (because  $\Delta_{2e} < 0$ ), corresponding to an optically thicker medium, while an atom in  $|3\rangle$  sees a positive potential (because  $\Delta_{3e} < 0$ ), corresponding to an optically thinner medium. Hence an atom will experience a  $\pi$  phase shift only if it is reflected in  $|2\rangle$ .

This phase shift can be converted into a population difference between the hyperfine levels. For that purpose two microwave  $\pi/2$  pulses resonant with the hyperfine transition are applied. They form a Ramsey scheme as shown in Fig. 3b. The atom is initially prepared in state  $|2\rangle$ . Then a microwave  $\pi/2$  pulse is applied, converting the internal state to the superposition state  $(|3\rangle + |2\rangle)/\sqrt{2}$ . After this, the atom interacts with the standing light wave. As explained above, the atom will experience a  $\pi$  phase shift only if it is reflected and in state  $|2\rangle$ . Thus the internal state of the reflected beam is changed to  $(|3\rangle + |2\rangle)/\sqrt{2}$ , while the internal state of the transmitted beam is not affected. As a result, there is an entanglement created between the internal and the external degree of freedom of the atom. The state vector of the system becomes:

$$|\psi\rangle \propto |\psi_B\rangle \otimes (|3\rangle - |2\rangle) + |\psi_C\rangle \otimes (|3\rangle + |2\rangle) \quad (1)$$

where  $|\psi_B\rangle$  and  $|\psi_C\rangle$  describe the centre-of-mass motion for the reflected and transmitted beams (see Fig. 1), respectively. This entanglement is the crucial point for the storage of information. The second microwave pulse acting on both beams (the transmitted and the reflected), converts the internal state of the transmitted beam to state  $|3\rangle$ , while the reflected beam is converted to state

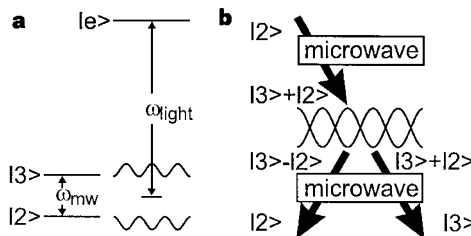


**Figure 3** Storage of which-way information. **a**, Left, simplified level scheme of  $^{85}\text{Rb}$ . The excited state ( $5^2P_{3/2}$ ) is labelled  $|e\rangle$ . The ground state ( $5^2S_{1/2}$ ) is split into two hyperfine states with total angular momentum  $F = 2$  and  $F = 3$ , which are labelled  $|2\rangle$  and  $|3\rangle$ , respectively. Right, the standing light wave with angular frequency  $\omega_{\text{light}}$  induces a light shift for both ground states which is drawn as a function of position. **b**, The beam splitter produces a phase shift that depends on the internal and external degree of freedom. A Ramsey scheme, consisting of two microwave  $\pi/2$  pulses, converts this phase shift into a population difference (see text).

$-|2\rangle$ . Thus, the state vector after the pulse sequence shown in Fig. 3b becomes:

$$|\psi\rangle \propto -|\psi_B\rangle \otimes |2\rangle + |\psi_C\rangle \otimes |3\rangle \quad (2)$$

We note that momentum transfer from the microwave slightly changes  $|\psi_B\rangle$  and  $|\psi_C\rangle$ , but this has negligible effects, as will be discussed below.

Equation (2) shows that the internal state is correlated with the way taken by the atom. The which-way information can be read out later by performing a measurement of the internal atomic state. The result of this measurement reveals which way the atom took: if the internal state is found to be  $|2\rangle$ , the atom moved along beam B, otherwise it moved along beam C.

A detailed calculation of the beam splitter reveals an additional phase shift, not discussed so far. It arises because the atoms travel in the light shift potential during  $t_{\text{Bragg}}$ . This creates a phase shift for the atoms proportional to  $U_0 \times t_{\text{Bragg}}$ , resulting in a relative phase shift between atoms in states  $|2\rangle$  and  $|3\rangle$ . Fortunately, this phase shift is identical for the transmitted and reflected beams and therefore does not affect the storing process in an essential manner. Moreover, a small detuning of the microwave frequency from the atomic resonance allows us to compensate for this effect, so that the simple model discussed above is valid.

### Interferometer with which-way information

After considering a single beam splitter, we now return to the complete interferometer. Sandwiching the first Bragg beam splitter between two microwave  $\pi/2$  pulses stores the which-way information in the internal atomic state, as described above. We note that the second Bragg beam splitter does not change the internal state.

Will there still be interference fringes in the far field, when the which-way information is stored? The experimental result is shown in Fig. 4: there are no fringes. The data were recorded with the same parameters as in Fig. 2a. The only difference is that two microwave pulses were added to store the which-way information. Atoms in both hyperfine states were detected, so that the which-way detector was not read out. The mere fact that which-way information is stored in the detector and could be read out already destroys the interference pattern. We have verified experimentally that the fringes also disappear when the which-way detector is read out, that is, when only atoms in state  $|2\rangle$  or only atoms in state  $|3\rangle$  are detected. Of course, the absolute size of the signal is reduced by a factor of two in these cases.

### Mechanical effects

We now discuss whether the loss of interference can be explained by mechanical effects of the which-way detector on the atomic

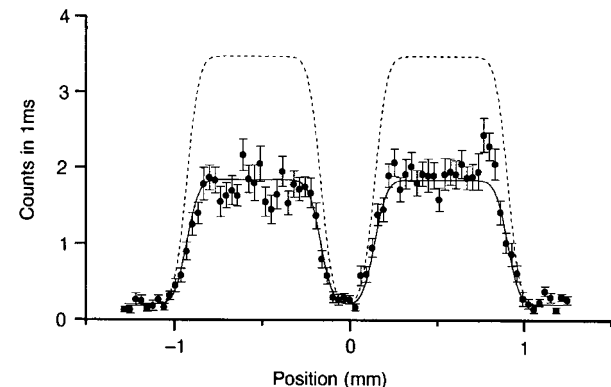


**Figure 4** Same as Fig. 2a, but with which-way information stored in the internal atomic state. The interference fringes are lost due to the storage of which-way information.

centre-of-mass motion. Therefore the transverse momentum transfer in the microwave field and the longitudinal displacement of the atomic wavefunction must be investigated.

To wash out the interference fringes, the transverse momentum transfer must have a distribution whose spread must correspond to at least half a fringe period. Such a “classical” momentum transfer distribution would also broaden the envelope of the fringe pattern by the same amount<sup>11</sup>. Comparing the experimental data in Fig. 2a and Fig. 4, it is obvious that the width of the envelope is not changed. This experimental result clearly shows that there is no significant transfer of transverse momentum in the microwave field.

The momentum transfer during the interaction with the microwave field can also be estimated theoretically. The microwave field is a standing wave diffracting the atomic beam. Because the atoms are travelling much less than a microwave wavelength during the interaction, the Raman–Nath approximation is valid. For a plane atomic wave, the probability to pick up  $n$  photon momenta during a  $\pi/2$  pulse is  $J_n^2(\pi/2)$ , where  $J_n$  is the  $n$ th order Bessel function<sup>16</sup>. Hence the probability of transferring more than two microwave photon momenta is less than 1%. The absorption of a single microwave photon shifts the position of the atom in the detector plane by 5 nm. It follows that the mechanical recoils during the interaction with the microwave field can shift the pattern by at most  $\pm 10$  nm—too small to be observed. Of course, the transverse width of the atomic beam is much less than a microwave wavelength, so that the atomic beam is not a plane wave. However, the atomic beam is a superposition of plane waves. The above Raman–Nath calculation applies for each plane wave component, so that the spread of the atomic beam cannot be larger than for a plane wave.

The second mechanical effect that could explain the loss of interference is a longitudinal displacement of the atomic wavefunction, as discussed in ref. 7. In our experiment, this argument does not apply, because the whole interaction sequence is pulsed. The atom’s potential energy varies as a function of time, not as a function of longitudinal position, so that the interaction does not create any longitudinal forces and displacements.

We conclude that the “classical” mechanical effects of the which-way detector on the atomic centre-of-mass motion are negligible, so that some other mechanism must enforce the loss of interference fringes.

### Correlations destroy interference

In order to investigate why the interference is lost, we consider the state vector for the interaction sequence used in Fig. 4. The state vector after the interaction with the first beam splitter sandwiched between the two microwave pulses is given in equation (2). The second beam splitter transforms this state vector into:

$$|\psi\rangle \propto -|\psi_D\rangle \otimes |2\rangle + |\psi_E\rangle \otimes |3\rangle + |\psi_F\rangle \otimes |2\rangle + |\psi_G\rangle \otimes |3\rangle \quad (3)$$

The sign of  $|\psi_F\rangle$  is positive due to the  $\pi$  phase shift during the reflection from the second beam splitter.

In the far field, the atomic position distribution under the left peak of the envelope is given by:

$$P(z) \propto |\psi_D(z)|^2 + |\psi_E(z)|^2 - \psi_D^*(z)\psi_E(z)\langle 2|3\rangle - \psi_E^*(z)\psi_D(z)\langle 3|2\rangle \quad (4)$$

because here the spatial wavefunctions  $\psi_F(z)$  and  $\psi_G(z)$  vanish. The first two terms describe the mean intensity under the envelope. Interference could only be created by the last two terms, but they vanish because  $\langle 2|3\rangle = 0$ . Precisely the same entanglement that was required to store the which-way information is now responsible for the loss of interference. In other words: the correlations between the which-way detector and the atomic motion destroy the interference, as discussed in ref. 3.

This loss of interference manifests itself as a dramatic change in the momentum distribution when adding the microwave fields to the interferometer, even though the microwave itself does not transfer enough momentum to the atom to wash out the fringes.

However, the addition of the microwave fields modifies the probability for momentum transfer by the light fields. This modification of the momentum transfer probability is due to the correlations between the which-way detector and the atomic motion.

Correlations between the interfering particle and the detector system are produced in any which-way scheme, for example, in the previously mentioned *gedanken* experiments of Einstein’s recoilless slit and Feynman’s light microscope. But in these experiments “classical” mechanical effects of the detector on the particle’s motion can explain the loss of interference as well, so that the effect of the correlations is hidden.

So far, the microwave field has been treated as a classical field, that is, not as a quantized field. At first glance this might seem to be unjustified, because the population difference between the two hyperfine states corresponds to the absorption of one microwave photon, so that the system also becomes entangled with the microwave field. Hence the interference terms in equation (4) must include an additional factor  $\langle\alpha|\beta\rangle$ , where  $|\alpha\rangle$  denotes the initial state of the microwave field, which changes to  $|\beta\rangle$  due to the absorption of one photon. In our experiment, the initial state  $|\alpha\rangle$  is a coherent state with a large mean photon number, and therefore the spread of the photon number is also large. It follows that  $\langle\alpha|\beta\rangle \approx 1$ , so that the entanglement with the microwave field has negligible effects, as has already been pointed out in ref. 3.

### Uncertainty relation

We now discuss the role of Heisenberg’s position–momentum uncertainty relation in our experiment. For this discussion it is essential that the two ways through the interferometer (beams B and C in Fig. 1) are never separated in transverse position space. This is because the beams have a transverse width of 450  $\mu\text{m}$  (as determined by the width of the lower collimation slit), but are shifted transversely only by a few micrometres (given by  $d$ ) with respect to each other. This has an important consequence: the storage of which-way information does not imply any storage of transverse position information.

Moreover, the atom is not localized with a precision of the order of  $d$  at any stage of the experiment. In particular, the atom stays delocalized during its whole passage through the interaction region, regardless of whether the microwave is on or off. Heisenberg’s position–momentum uncertainty relation could only be invoked if the atom were localized. Hence the uncertainty relation does not imply any back action onto the transverse momentum, either “classical” or “quantum”.

Of course, in every real experiment there are localization effects due to the finite size of the apparatus. This localization leads to a back action onto the momentum. But this back action is not at all related to the fringe separation. For example, in our set-up the atoms are localized within one wavelength of the microwave. The corresponding back action onto the transverse momentum implied by the uncertainty relation is of the order of one microwave photon recoil and has been analysed above. This back action is four orders of magnitude smaller than the fringe separation, so that it cannot explain the loss of interference. Hence correlations can explain the loss of interference, while the uncertainty relation cannot. This answers the controversial question cited in the introduction: complementarity is not enforced by the uncertainty relation.

This result is not in conflict with the results of Wiseman *et al.*<sup>11</sup>, who considered only “experiments in which double-slit interference patterns are destroyed by making a position measurement”<sup>11</sup>. In our experiment, no double slit is used and no position measurement is performed, so that the results of ref. 11 do not apply. It is an open question whether the concept of “quantum” momentum transfer can be generalized to schemes without a mechanical double slit. Such a generalization would have to take into account the fact that in our experiment, the amount of momentum transferred by the light fields is always either zero or exactly  $2\hbar k_{\text{light}}$ .

Although beams B and C are never separated in transverse position space, they are separated in transverse momentum space. The separation is  $2\hbar k_{\text{light}}$ , as is required for first-order Bragg reflection. Storing which-way information therefore corresponds to storing transverse momentum information with an accuracy of the order of  $\Delta p_z \approx \hbar k_{\text{light}}$ . So the uncertainty relation implies that the storing process must include a back action onto the transverse position of the order of  $\Delta z \approx \lambda_{\text{light}}$ . This back action is due to the following effect. In the Bragg regime, the interaction time with the standing light wave,  $t_{\text{Bragg}}$ , is so long that the atoms move at least a transverse distance of the order of  $\lambda_{\text{light}}/2$  within  $t_{\text{Bragg}}$ . In a naive picture, the atoms can be Bragg-reflected at the beginning or at the end of this interaction, which implies a transverse position uncertainty of the order of  $\Delta z \approx \lambda_{\text{light}}$ . But this back action onto the near-field position cannot destroy the far-field fringe pattern. The interference pattern created in the interferometer is a pattern in momentum space, not in position space. The far-field position distribution is simply a picture of the final momentum distribution.  $\square$

Received 3 February; accepted 15 June 1998.

1. Bohr, N. in *Albert Einstein: Philosopher-Scientist* (ed. Schilpp, P. A.) 200–241 (Library of Living Philosophers, Evanston, 1949); reprinted in *Quantum Theory and Measurement* (eds Wheeler, J. A. & Zurek, W. H.) 9–49 (Princeton Univ. Press, 1983).
2. Feynman, R., Leighton, R. & Sands, M. in *The Feynman Lectures on Physics* Vol. III, Ch. I (Addison Wesley, Reading, 1965).

3. Scully, M. O., Englert, B. G. & Walther, H. Quantum optical tests of complementarity. *Nature* **351**, 111–116 (1991).
4. Haroche, S. in *High-resolution Laser Spectroscopy* (ed. Shimoda, K.) 253–313 (Topics in Applied Physics, Vol. 13, Springer, 1976).
5. Rauch, H. *et al.* Verification of coherent spinor rotation of fermions. *Phys. Lett. A* **54**, 425–427 (1975).
6. Badurek, G., Rauch, H. & Tuppinger, D. Neutron interferometric double-resonance experiment. *Phys. Rev. A* **34**, 2600–2608 (1986).
7. Storey, P., Tan, S., Collett, M. & Walls, D. Path detection and the uncertainty principle. *Nature* **367**, 626–628 (1994).
8. Englert, B. G., Scully, M. O. & Walther, H. Complementarity and uncertainty. *Nature* **375**, 367–368 (1995).
9. Storey, E. P., Tan, S. M., Collett, M. J. & Walls, D. F. Complementarity and uncertainty. *Nature* **375**, 368 (1995).
10. Wiseman, H. & Harrison, F. Uncertainty over complementarity? *Nature* **377**, 584 (1995).
11. Wiseman, H. M. *et al.* Nonlocal momentum transfer in Welch wave measurements. *Phys. Rev. A* **56**, 55–75 (1997).
12. Eichmann, U. *et al.* Young's interference experiment with light scattered from two atoms. *Phys. Rev. Lett.* **70**, 2359–2362 (1993).
13. Cohen-Tannoudji, C. Effect of non-resonant irradiation on atomic energy levels. *Metrologia* **13**, 161–166 (1977); reprinted in Cohen-Tannoudji, C. *Atoms in Electromagnetic Fields* 343–348 (World Scientific, London, 1994).
14. Kunze, S., Dürr, S. & Rempe, G. Bragg scattering of slow atoms from a standing light wave. *Europhys. Lett.* **34**, 343–348 (1996).
15. Kunze, S. *et al.* Standing wave diffraction with a beam of slow atoms. *J. Mod. Opt.* **44**, 1863–1881 (1997).
16. Bernhardt, A. F. & Shore, B. W. Coherent atomic deflection by resonant standing waves. *Phys. Rev. A* **23**, 1290–1301 (1981).

**Acknowledgements.** We thank S. Kunze for discussions. This work was supported by the Deutsche Forschungsgemeinschaft.

Correspondence and requests for materials should be addressed to G.R. (e-mail: gerhard.rempe@uni-konstanz.de).

# A critical window for cooperation and competition among developing retinotectal synapses

Li I. Zhang\*, Huizhong W. Tao\*, Christine E. Holt†, William A. Harris† & Mu-ming Poo

Department of Biology, University of California at San Diego, La Jolla, California 92093-0357, USA

\* These authors contributed equally to this work.

**In the developing frog visual system, topographic refinement of the retinotectal projection depends on electrical activity. *In vivo* whole-cell recording from developing *Xenopus* tectal neurons shows that convergent retinotectal synapses undergo activity-dependent cooperation and competition following correlated pre- and postsynaptic spiking within a narrow time window. Synaptic inputs activated repetitively within 20 ms before spiking of the tectal neuron become potentiated, whereas subthreshold inputs activated within 20 ms after spiking become depressed. Thus both the initial synaptic strength and the temporal order of activation are critical for heterosynaptic interactions among convergent synaptic inputs during activity-dependent refinement of developing neural networks.**

Electrical activity in the developing nervous system plays a crucial role in the establishment of early nerve connections<sup>1,2</sup>. In the mammalian visual system, both the formation of ocular dominance columns in the primary visual cortex<sup>3–5</sup> and the segregation of retinal ganglion axons into eye-specific layers in the lateral geniculate nucleus<sup>6</sup> depend on electrical activity in the visual pathways. The pattern of activity in the optic nerves seems to serve an instructive role, as synchronous stimulation of optic nerves abolishes the formation of ocular dominance columns, whereas asynchronous stimulation leads to sharp ocular dominance columns<sup>7</sup>. Artificially synchronized activity in the optic nerve also disrupts the development of orientation tuning in the visual cortex<sup>8</sup>. In the visual system of frog, chick and fish, retinal axons use activity-independent mechanisms initially to establish a topographic map,

but the initial map is coarse and terminals from each retinal axon arborize over a large portion of the tectum. During development, the map becomes refined as retinal axons progressively restrict their arborizations to a smaller fraction of the tectum<sup>9,10</sup>. Topographic refinement of the retinotectal projection also depends on activity patterns, as this process is impaired when retinal activity is blocked or uniformly synchronized by raising the animals in strobe light<sup>11–14</sup>. Thus, throughout the visual system, the refinement of connections depends on the pattern of activity, but the underlying physiological mechanisms are largely unknown.

We have examined quantitatively the effects of activity patterns on the strength of developing central synapses in the *Xenopus* retinotectal system. *In vivo* whole-cell recordings were made from neurons in the optic tectum of young *Xenopus* tadpoles to monitor changes in the strength of retinotectal synapses following repetitive electrical stimulation of retinal neurons in the contralateral eye. By

† Present address: Department of Anatomy, University of Cambridge, Cambridge CB2 3DY, UK.